Differential requirements for the chemokine receptor CCR7 in T cell activation during *Listeria monocytogenes* infection

Mischo Kursar,[1] Uta E. Höpken,[2] Markus Koch,[1] Anne Köhler,[1] Martin Lipp,[2] Stefan H.E. Kaufmann,[1] and Hans-Willi Mittrücker[1]

[1]Department of Immunology, Max-Planck Institute for Infection Biology, 10117 Berlin, Germany
[2]Department for Molecular Tumor Genetics and Immunogenetics, Max-Delbrück Center for Molecular Medicine, 13092 Berlin, Germany

Effective priming of T cell responses depends on cognate interactions between naive T cells and professional antigen-presenting cells (APCs). This contact is the result of highly coordinated migration processes, in which the chemokine receptor CCR7 and its ligands, CCL19 and CCL21, play a central role. We used the murine *Listeria monocytogenes* infection model to characterize the role of the CCR7/CCR7 ligand system in the generation of T cell responses during bacterial infection. We demonstrate that efficient priming of naive major histocompatibility complex (MHC) class Ia–restricted $CD8^+$ T cells requires CCR7. In contrast, MHC class Ib–restricted $CD8^+$ T cells and MHC class II–restricted $CD4^+$ T cells seem to be less dependent on CCR7; memory T cell responses are independent of CCR7. Infection experiments with bone marrow chimeras or mice reconstituted with purified T cell populations indicate that CCR7 has to be expressed on $CD8^+$ T cells and professional APCs to promote efficient MHC class Ia–restricted T cell priming. Thus, different T cell subtypes and maturation stages have discrete requirements for CCR7.

CORRESPONDENCE
Hans-Willi Mittrücker:
mittruecker@
mpiib-berlin.mpg.de

Abbreviations used: CFSE, carboxyfluorescein succinimidyl ester; f-met, formyl-methionine; LLO, listeriolysin O; LmOVA, recombinant *Listeria monocytogenes* strain secreting a truncated OVA protein; MACS, magnetic cell sorting; TSB, tryptic soy broth.

Close contact between naive T cells and professional APCs is a prerequisite for effective T cell priming. This contact does not occur randomly, but rather is a consequence of highly coordinated migration processes which involve different adhesion molecules and chemokine/chemokine receptor systems. The chemokine receptor CCR7, and its ligands, CCL19 (EBV-induced gene 1 ligand chemokine, macrophage inflammatory protein-3β) and CCL21 (secondary lymphoid tissue chemokine, 6Ckine), seem to play a central role (1, 2). CCR7 is expressed on naive T cells, a subpopulation of memory T cells, and B cells (1). Immature dendritic cells do not express CCR7; however, during maturation, CCR7 is up-regulated on their surface (3). CCL19 and CCL21 are secreted by stromal cells that are located in the T cell zones of secondary lymphoid organs. In addition, CCL21 is expressed by high endothelial venules and the lymphatic endothelium (1, 2, 4). Standard laboratory mouse strains express at least two isoforms of CCL21—CCL21-Ser and CCL21-Leu—which are encoded by independent genes. In contrast to CCL21-Ser, expression of CCL21-Leu is restricted to the lymphatic epithelium of peripheral tissues (4). After chemokine attraction, naive T cells and activated dendritic cells enter lymphoid tissues and migrate along the CCL19/CCL21 gradients into T cell zones, where cognate interactions eventually occur (1, 2, 5).

The concept of chemokine-controlled T cell priming is supported by observations in CCR7-deficient mice and in *plt* (paucity of lymph node T cell) mice, which fail to express CCL19 and CCL21-Ser and show impaired expression levels of CCL21-Leu (4, 6–9). In both mouse strains, T lymphocytes home poorly into lymph nodes and Peyer's patches, and inside lymph nodes, T cells are distributed aberrantly (4, 6, 8). Although T cells can still enter the spleen, these mice fail to develop distinct T cell zones in the white pulp (4, 6). Furthermore, migration of mature dendritic cells into secondary lymphoid tissues is impaired (3, 6). Consequently, both mouse strains demonstrate altered acquired immune responses. In CCR7-deficient mice, delayed-type hypersensitivity reactions are reduced, and T cell dependent antibody production is delayed (6). CCR7 mice fail to reject allogeneic tumors and rejec-

tion of grafted allogeneic hearts is delayed (9). In *plt* mice, acquired immune responses seem to be affected less severely. Although, *plt* mice are more susceptible to infection with murine hepatitis virus (7), immune responses after infection with lymphocytic choriomeningitis virus, vesicular stomatitis virus, and different strains of vaccinia virus are similar to that

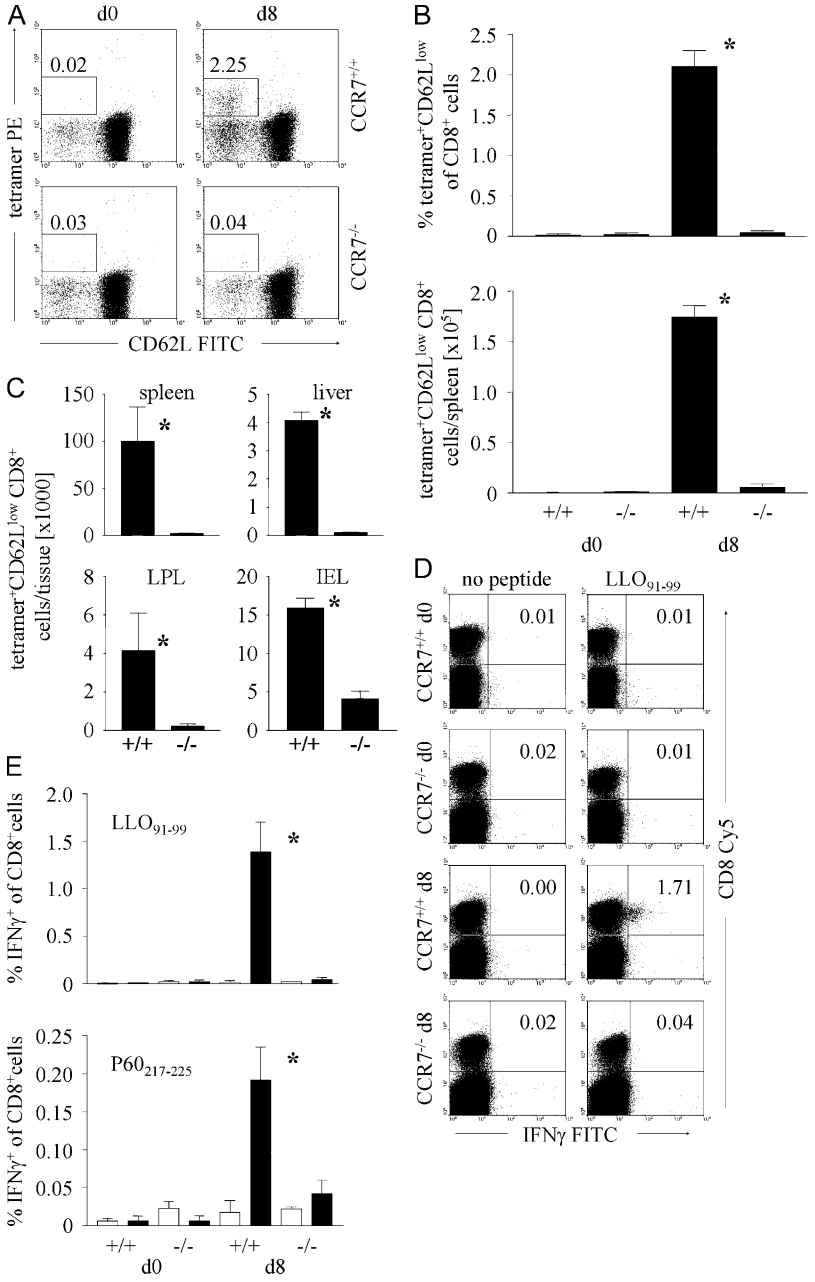

Figure 1. CD8⁺ T cell response to primary *L. monocytogenes* infection. CCR7$^{+/+}$ and CCR7$^{-/-}$ mice on BALB/c background were infected i.v. with 10^3 (A, B, D, E) or orally with 10^9 *L. monocytogenes* organisms (C). After 8 d, spleen cells (A, B) or cells isolated from liver, lamina propria, and epithelium of the small intestine (C) were stained with FITC-conjugated anti-CD62L mAb, Cy5-conjugated anti-CD8α mAb, and PE-conjugated LLO_{91-99} tetramers. Cells were analyzed by flow cytometry after the addition of propidium iodide. (A) CD8-gated representative results. Numbers give the percent of cells within the region and are calculated for CD8⁺ T cells only. (B, C) The percent of LLO_{91-99}-tetramer⁺ CD62L^{low} of CD8⁺ T cells and absolute number of LLO_{91-99}-tetramer⁺ CD62L^{low} CD8⁺ T cells per spleen (mean ± SD of three independently analyzed mice per group). In addition, spleen cells were incubated for 5 h with the peptides LLO_{91-99} or $p60_{217-225}$ (D, E). Cells were stained extracellularly with anti-CD8α mAb and intracellularly with anti-IFNγ mAb and analyzed by flow cytometry. (D) Representative results. Numbers give the frequencies for IFNγ⁺ of CD8⁺ cells only. (E) Frequencies of IFNγ⁺ cells among CD8⁺ T cells after in vitro incubation without (white bars) or with peptides LLO_{91-99} or $p60_{217-225}$ (black bars; mean ± SD of three individually analyzed mice per group). *Difference between cells from infected CCR7$^{+/+}$ and CCR7$^{-/-}$ mice was statistically significant ($P < 0.05$).

in control mice (8). Despite an aberrant T cell migration pattern in infected *plt* mice, antiviral T cell and antibody responses are virtually normal, and *plt* mice can control viral infections (8). Furthermore, immunization of *plt* mice with ovalbumin results in delayed, but otherwise normal or even stronger priming of $CD4^+$ T cells (4). Overall, these studies question the general requirement for CCR7/CCR7 ligands interactions for T cell priming and point to more complex functions during acquired immune responses.

Infection of mice with the intracellular bacterium *Listeria monocytogenes* represents a valuable model to study T cell responses in vivo (10, 11). After infection, *L. monocytogenes* migrate to their main target organs—spleen and liver—where they invade macrophages and hepatocytes. In these cells, *L. monocytogenes* penetrate the phagosomal membrane and enter the cytoplasm. Because of their intracytoplasmic habitat, *L. monocytogenes*–derived antigens are presented efficiently via the MHC class I pathway; this results in the induction of a potent $CD8^+$ T cell response. $CD8^+$ T cells are crucial for the control of *L. monocytogenes* infection and are responsible for protection against reinfection. In addition, a considerable $CD4^+$ T cell response is induced, although the role of this cell population is less clear (12, 13). Several *L. monocytogenes*–derived T cell epitopes have been characterized, including MHC class Ia–, MHC class Ib–, and MHC class II–presented peptides (10, 14). The respective peptides have been used extensively to study the kinetics and regulation of *L. monocytogenes*–specific T cell responses during infection. These analyses yielded extensive information on the effector and memory phases of *L. monocytogenes*–specific $CD4^+$ and $CD8^+$ T cell responses. However, the early events of T cell priming remain largely unknown. Only limited information is available on the sites and the APC populations that are involved in T cell priming and the requirements for T cell differentiation into effector and memory cells (15–18).

We analyzed CCR7-deficient mice using the murine *L. monocytogenes* infection model. We demonstrate that CCR7 has to be expressed on $CD8^+$ T cells and professional APCs to allow efficient MHC class Ia–restricted priming. In contrast, MHC class Ib–restricted $CD8^+$ T cells and MHC class II–restricted $CD4^+$ T cells are less dependent, and memory T cell responses are independent of CCR7.

RESULTS

$CCR7^{-/-}$ mice backcrossed onto the BALB/c background and $CCR7^{+/+}$ BALB/c control mice were i.v. infected with 10^3 *L. monocytogenes* organisms, and the $CD8^+$ T cell response was analyzed using H-$2K^d$ tetramers loaded with the immunodominant peptide listeriolysin O $(LLO)_{91–99}$ (19). 8 d after infection, approximately 2% of all $CD8^+$ splenocytes from $CCR7^{+/+}$ mice were $LLO_{91–99}$ tetramer$^+$ (Fig. 1, A and B). Spleens of $CCR7^{+/+}$ mice contained a total of 1.5–2.0×10^5 $LLO_{91–99}$ tetramer$^+$ $CD8^+$ T cells. In contrast, frequencies and numbers of $LLO_{91–99}$ tetramer$^+$ $CD8^+$ T cells in infected $CCR7^{-/-}$ mice were reduced and were close to background levels that were observed in noninfected animals (Fig. 1, A and B). The impaired response in $CCR7^{-/-}$ mice was not restricted to the spleen. After oral infection, we observed reduced cell numbers of $LLO_{91–99}$ tetramer$^+$ $CD8^+$ T cells in spleen, liver, and lamina propria and epithelium of the small intestine (Fig. 1 C). Similar results were obtained at d 9, 10, and 17 after infection, excluding that the low frequencies of $LLO_{91–99}$ tetramer$^+$ $CD8^+$ T cells were the result of a delayed T cell response in $CCR7^{-/-}$ mice (unpublished data).

In parallel to the tetramer assay, splenocytes from infected $CCR7^{+/+}$ and $CCR7^{-/-}$ BALB/c mice were restimulated in vitro with the peptides $LLO_{91–99}$ and $p60_{217–225}$, an independent immunodominant *L. monocytogenes*–derived $CD8^+$ T cell epitope (19). Stimulation with both peptides induced IFNγ production in $CD8^+$ spleen cells from infected control mice (Fig. 1, D and E). In contrast, only marginal frequencies of IFNγ^+ $CD8^+$ T cells were observed in spleens of $CCR7^{-/-}$ mice; this confirmed the results from the $LLO_{91–99}$ tetramer assay and indicated that the impaired response was not restricted to the $LLO_{91–99}$ epitope.

Despite the marginal proportion of *L. monocytogenes*–specific $CD8^+$ T cells, $CCR7^{-/-}$ mice tolerated the *L. monocytogenes* inoculum that was used in our experiments, and susceptibility to infection was not increased substantially. $CCR7^{-/-}$ mice showed impaired clearance of *L. monocytogenes* with slightly higher bacterial titers at late time points after infection (Fig. 2). However, at later time points (>10 d after infection), $CCR7^{+/+}$ and $CCR7^{-/-}$ mice usually had cleared *L. monocytogenes* from spleen and liver (unpublished data).

Infection of mice with *L. monocytogenes* results in the generation of specific $CD8^+$ memory T cells, which mount an accelerated and elevated anti–*L. monocytogenes* T cell response to reinfection. To assess the role of CCR7 in the

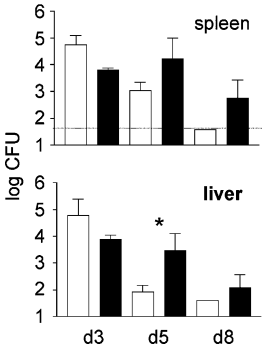

Figure 2. Bacterial burdens in spleen and liver of $CCR7^{-/-}$ mice after *L. monocytogenes* infection. $CCR7^{+/+}$ (white bars) and $CCR7^{-/-}$ mice (black bars) were i.v. infected with 10^3 *L. monocytogenes* organisms. On the indicated days, mice were killed and bacterial titers in spleen and liver were determined. Results represent the mean ± SD of four or five mice per group. The dotted line gives the detection limit of our assay (40 bacteria/organ). *Difference between titers from infected $CCR7^{+/+}$ and $CCR7^{-/-}$ mice was statistically significant ($P < 0.05$).

generation and maintenance of $CD8^+$ memory T cells, $CCR7^{+/+}$ and $CCR7^{-/-}$ BALB/c mice were infected with 10^3 *L. monocytogenes* organisms; 6 wk later, mice were challenged with 10^5 *L. monocytogenes* organisms. 6 d after secondary infection, $CD8^+$ T cell responses were analyzed with $LLO_{91–99}$ tetramers and by intracellular cytokine staining after in vitro restimulation with $LLO_{91–99}$ or $p60_{217–225}$ peptides (Fig. 3). $CCR7^{+/+}$ control mice demonstrated enhanced frequencies and absolute numbers of $LLO_{91–99}$- and $p60_{217–225}$-specific $CD8^+$ T cells, characteristic for secondary responses. Despite the marginal primary responses, $CD8^+$ T cell frequencies and total numbers in secondary infected $CCR7^{-/-}$ mice were similar to those in $CCR7^{+/+}$ control animals. As could be expected from the strong secondary $CD8^+$ T cell response, all $CCR7^{+/+}$ and $CCR7^{-/-}$ animals had cleared the infection from spleen and liver at the time point of T cell analysis. Direct measurement of $LLO_{91–99}$-specific $CD8^+$ memory T cells 6 to 8 wk after infection was difficult, because even in $CCR7^{+/+}$ mice, numbers of memory cells in spleen and liver were close to the detection level of our assay (unpublished data). To circumvent this problem, we used a recombinant *L. monocytogenes* strain that secretes a truncated OVA protein (LmOVA) (20). Infection of C57BL/6 mice with LmOVA results in a substantial $CD8^+$ T cell response to the $OVA_{257–264}$-epitope and a high level of $CD8^+$ memory T cells (21). As expected, we observed a strong $OVA_{257–264}$-specific $CD8^+$ T cell response in $CCR7^{+/+}$ C57BL/6 mice, but only a weak response in $CCR7^{-/-}$ C57BL/6 mice (Fig. 4 A). Reinfection of mice caused an extensive secondary $OVA_{257–264}$-specific $CD8^+$ T cell response, which was reduced only slightly in $CCR7^{-/-}$ mice compared with $CCR7^{+/+}$ mice (Fig. 4 B). Analysis of $CD8^+$ T cells from spleen and liver of mice 2 mo after LmOVA infection revealed that both mouse strains had generated $OVA_{257–264}$-specific memory T cells, although the frequencies and numbers of these cells were reduced in $CCR7^{-/-}$ mice (Fig. 4 C).

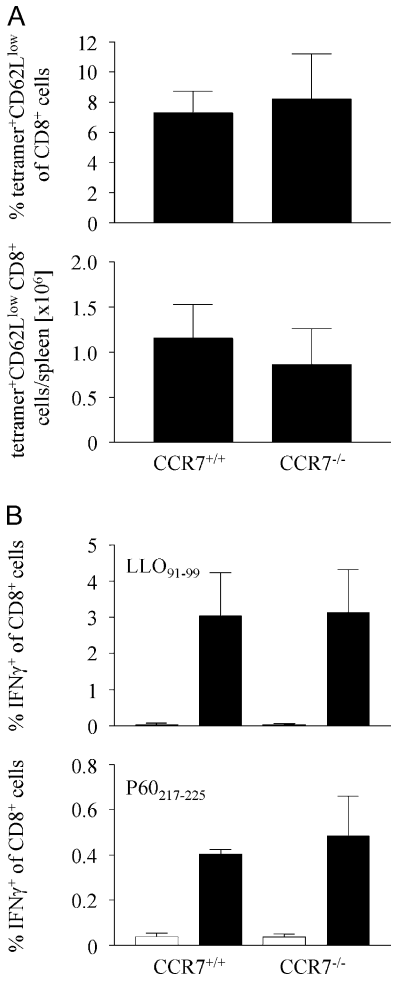

Figure 3. $CD8^+$ T cell responses to $LLO_{91–99}$ or $p60_{217–225}$ after secondary *L. monocytogenes* infection. $CCR7^{+/+}$ and $CCR7^{-/-}$ mice on BALB/c background were infected i.v. with 10^3 *L. monocytogenes* organisms. After 44 d, mice were secondarily infected (i.v.) with 10^5 *L. monocytogenes* organisms. On day 6 after secondary infection, spleen cells were analyzed as described in Fig. 1. (A) Frequencies and absolute numbers of $LLO_{91–99}$-tetramer$^+$ $CD62L^{low}$ $CD8^+$ T cells in $CCR7^{+/+}$ and $CCR7^{-/-}$ BALB/c mice (mean ± SD of three individually analyzed mice per group). (B) Frequencies of IFNγ$^+$ cells among $CD8^+$ T cells after short-term incubation without (white bars) or with peptides $LLO_{91–99}$ or $p60_{217–225}$ (black bars; mean ± SD of three individually analyzed mice per group). There was no significant difference ($P > 0.05$) between $CCR7^{+/+}$ and $CCR7^{-/-}$ mice in frequencies and total cell numbers of $LLO_{91–99}$-tetramer$^+$ $CD62L^{low}$ $CD8^+$ T cells (A), and in the frequencies of IFNγ-producing cells after peptide restimulation (B).

In addition to $CD8^+$ T cell responses that are restricted by conventional MHC class Ia molecules, *L. monocytogenes* induces $CD8^+$ T cell responses that are restricted by MHC class Ib molecules (10). So far, three *L. monocytogenes*–derived formyl-methionine (f-met) peptides have been identified, which are recognized by H2-M3–restricted $CD8^+$ T cells (10). Because the H2-M3–restricted response is far more pronounced in C57BL/6 mice than in BALB/c mice (22), $CCR7^{-/-}$ mice backcrossed onto the C57BL/6 background were infected with 2×10^3 *L. monocytogenes* organisms. 8 d after infection, spleen cells were incubated for 5 h with a cocktail of the three *L. monocytogenes*–derived f-met peptides (fMIGWII, fMIVIL, and fMIVTLF); frequencies of IFNγ-producing $CD8^+$ T cells were determined by flow cytometry (Fig. 5). In infected control mice, f-met peptides induced IFNγ production in approximately 0.8% of the $CD8^+$ splenocytes; this corresponded to 10^5 f-met–restricted $CD8^+$ T cells per spleen. Significant frequencies of f-met–restricted $CD8^+$ T cells also were present in spleens of infected $CCR7^{-/-}$ C57BL/6 mice. Although frequencies in

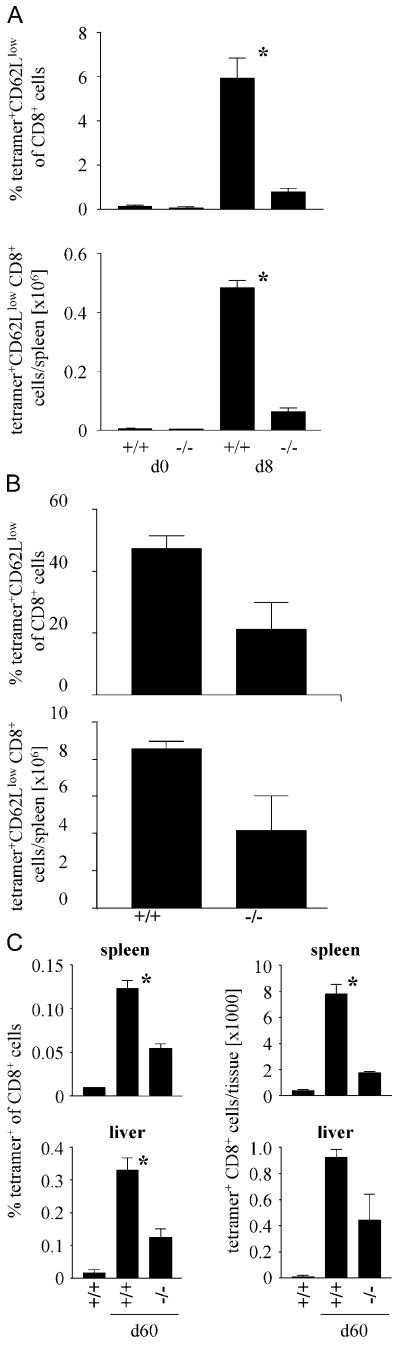

Figure 4. CD8$^+$ T cell response to OVA$_{257–264}$ after primary and secondary infection with LmOVA. CCR7$^{+/+}$ and CCR7$^{-/-}$ mice on C57BL/6 background were infected i.v. with 5×10^3 LmOVA organisms and 60 d later were challenged i.v. with 10^5 LmOVA organisms. 8 d after primary infection (A) and 6 d after secondary infection (B), frequencies and numbers of OVA$_{257–264}$-specific CD8$^+$ T cells were determined in spleens of infected mice. (C) Frequencies and numbers of OVA$_{257–264}$-specific CD8$^+$ memory T cells in spleen and liver were measured 60 d after primary infection of mice. For comparison, we show values for naive CCR7$^{+/+}$ animals. Mean ±SD of three individually analyzed mice per group. *Difference between infected CCR7$^{+/+}$ and CCR7$^{-/-}$ mice was statistically significant ($P < 0.05$).

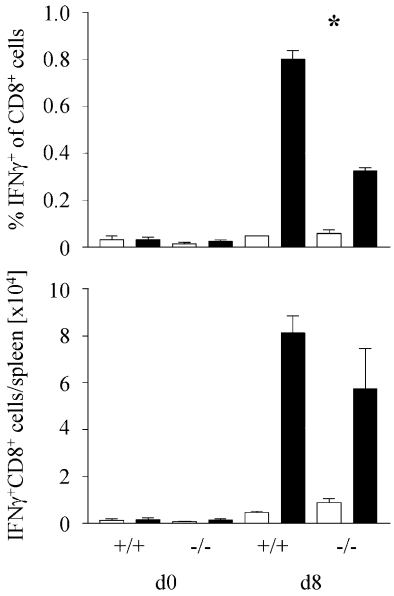

Figure 5. CD8$^+$ T cell response to f-met peptides during primary infection. CCR7$^{+/+}$ and CCR7$^{-/-}$ mice on C57BL/6 background were i.v. infected with 2×10^3 *L. monocytogenes* organisms. After 8 d, spleen cells were incubated for 5 h with a cocktail of the f-met peptides fMIGWII, fMIVIL and fMIVTLF. Cells were stained extracellularly with anti-CD8α mAb and intracellularly with anti-IFNγ mAb and analyzed by flow cytometry. The figure shows frequencies of IFNγ$^+$ cells among CD8$^+$ T cells and total numbers of IFNγ$^+$ CD8$^+$ T cells per spleen after incubation without (white bars) and with peptides (black bars; mean ± SD of three individually analyzed mice per group). *Difference between IFNγ$^+$ cells from infected CCR7$^{+/+}$ and CCR7$^{-/-}$ mice after restimulation with peptide was statistically significant ($P < 0.05$).

CCR7$^{-/-}$ mice were reduced compared with controls, total numbers did not differ significantly between both mouse strains; this mainly was due to the enlarged spleen size of CCR7$^{-/-}$ mice (unpublished data). In two further experiments, we consistently observed similar or only slightly reduced numbers of f-met–specific CD8$^+$ T cells in CCR7$^{+/+}$ and CCR7$^{-/-}$ mice (unpublished data). Thus, the lack of CCR7 only marginally impaired f-met peptide–specific CD8$^+$ T cell responses during *L. monocytogenes* infection.

The immunodominant I-A^b-restricted epitope LLO$_{190–201}$ can be used for quantitative analysis of *L. monocytogenes*–specific CD4$^+$ T cell responses in C57BL/6 mice (12). CCR7$^{+/+}$ and CCR7$^{-/-}$ mice on C57BL/6 background were infected with *L. monocytogenes*; 10 d after infection, frequencies of LLO$_{190–201}$-restricted CD4$^+$ T cells were determined (Fig. 6). In infected CCR7$^{+/+}$ control mice, approximately 0.6% of CD4$^+$ splenocytes produced IFNγ in response to LLO$_{190–201}$. Infected CCR7$^{-/-}$ mice demonstrated similar frequencies and total numbers of responding cells (Fig. 6). When we analyzed CCR7$^{+/+}$ and CCR7$^{-/-}$ mice 8 or 9 d after infection, results were comparable (unpublished data). T cells from CCR7$^{+/+}$ mice showed a ho-

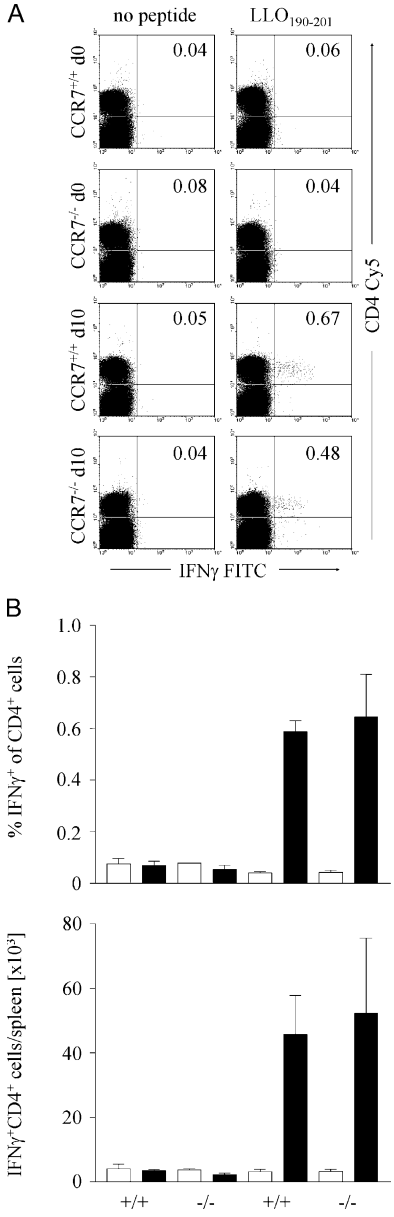

Figure 6. CD4$^+$ T cell response to LLO$_{190–201}$ during primary infection. CCR7$^{+/+}$ and CCR7$^{-/-}$ mice on C57BL/6 background were i.v. infected with 2×10^3 *L. monocytogenes* organisms. After 10 d, spleen cells were incubated for 5 h with the peptide LLO$_{190–201}$. Cells were stained extracellularly with anti-CD4 mAb and intracellularly with anti-IFNγ mAb, and analyzed by flow cytometry. (A) Representative results. (B) Frequencies of IFNγ^+ cells among CD4$^+$ T cells and absolute numbers of IFNγ^+ CD4$^+$ cells per spleen after incubation without (white bars) and with peptide LLO$_{190–201}$ (black bars; mean $\pm$ SD of three individually analyzed mice per group). There was no significant difference ($P > 0.05$) between IFNγ^+ cells from infected CCR7$^{+/+}$ and CCR7$^{-/-}$ mice after restimulation with peptide.

mogenous response in all six experiments, in which we analyzed CD4$^+$ T cell responses. In contrast, CD4$^+$ T cells from CCR7$^{-/-}$ mice demonstrated some variation. We observed individual mice, in which the response was reduced up to one third of the mean response of wild-type animals. However, in none of the experiments did the difference between the mean response in CCR7$^{+/+}$ and CCR7$^{-/-}$ mice reached a statistically significant level ($P < 0.05$). In summary, our results demonstrate that MHC class II–restricted CD4$^+$ T cell responses to *L. monocytogenes* are far less dependent on CCR7 than are the corresponding MHC class Ia–restricted CD8$^+$ T cell responses.

Because CCR7 is expressed on naive CD8$^+$ T cells and on activated dendritic cells, we determined the role of CCR7 on CD8$^+$ T cells in an adoptive T cell transfer model. CD8$^+$ T cells from the TCR-transgenic mouse strain OT1 recognize OVA$_{257–264}$, the immunodominant CD8$^+$ T cell epitope that is included in the truncated ovalbumin protein expressed by LmOVA (20). To determine whether CCR7 expression on CD8$^+$ T cells is sufficient for the induction of a response, purified CD8$^+$ T cells from OT1 donors were labeled with carboxyfluorescein succinimidyl ester (CFSE) and adoptively transferred into CCR7$^{+/+}$ and CCR7$^{-/-}$ recipients. After 24 h, mice were infected with LmOVA; 72 h later, proliferation of transferred CD8$^+$ T cells was analyzed by flow cytometry (Fig. 7). In noninfected CCR7$^{+/+}$ animals, transferred T cells maintained the CFSE^{high} phenotype. Infection of CCR7$^{+/+}$ recipients induced proliferation of CD8$^+$ donor cells as indicated by the stepwise loss of CFSE staining. In noninfected CCR7$^{-/-}$ recipients, we detected a low level of donor cell proliferation for which we currently have no explanation. However, proliferation did not increase further upon LmOVA infection. As was expected from the analysis of the endogenous CD8$^+$ T cell response to LmOVA infection (Fig. 4 A), the block in activation of transferred CD8$^+$ T cells was incomplete in CCR7$^{-/-}$ recipients. At day 4 after infec-

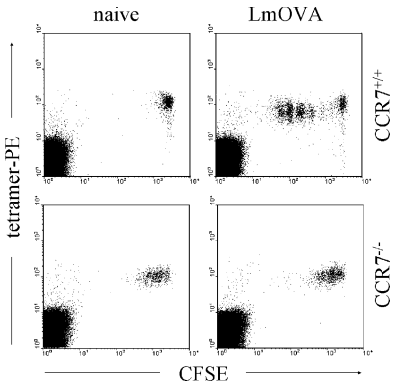

Figure 7. Expression of CCR7 on CD8$^+$ T cells is insufficient for T cell priming. CCR7$^{+/+}$ and CCR7$^{-/-}$ mice on C57BL/6 background received 4×10^6 purified CFSE-labeled CD8$^+$ T cells from OT1 mice. After 24 h, recipients were i.v. infected with 5×10^3 LmOVA organisms, or were left untreated (naive). 3 d later, spleen cells were stained with PE-conjugated OVA$_{257–264}$ tetramers and Cy5-conjugated anti-CD8α mAb, and CFSE expression on transferred CD8$^+$ T cells was analyzed by flow cytometry. Figures show CD8-gated T cells only and are representative for two individually analyzed mice per group.

tion, some proliferation of donor cells also was observed in $CCR7^{-/-}$ recipients (unpublished data).

In a complementary set of experiments, we generated bone marrow chimeras, in which $\alpha\beta TCR^+$ T cells had a $CCR7^{+/+}$ or a $CCR7^{-/-}$ genotype. A similar approach recently was described to analyze mutant B cells in a nonmutant environment (23). $TCR\beta^{-/-}$ mice were irradiated and reconstituted with bone marrow cells from $TCR\beta^{-/-}$ mice. In addition, these animals received bone marrow cells from either $CCR7^{+/+}$ or $CCR7^{-/-}$ mice at a 5:1 ratio of $TCR\beta^{-/-}/CCR7^{+/+}$or $TCR\beta^{-/-}/CCR7^{-/-}$. Because of this reconstitution protocol, the majority of hematopoietic cells in the chimeras had a $TCR\beta^{-/-}CCR7^{+/+}$ genotype. In contrast, $\alpha\beta TCR^+$ T cells were exclusively $CCR7^{+/+}$ or $CCR7^{-/-}$. To confirm the mixed chimerism, bone marrow cells of $TCR\beta^{-/-}$ mice that were reconstituted with $TCR\beta^{-/-}$ and $CCR7^{-/-}$ bone marrow were T cell depleted; DNA from these cells was analyzed by quantitative PCR for the ratio of $CCR7^{+/+}(TCR\beta^{-/-})/CCR7^{-/-}$ cells. 6 wk after reconstitution, we determined a ratio of 1:5.68 ± 0.74 ($n = 5$) for $CCR7^-/CCR7^+$ DNA, a value which was similar to the 1:5 ratio of bone marrow cells that was used for the original reconstitution. 8 wk after reconstitution, when mice showed normal T cell levels in the peripheral blood, the chimeras were infected with LmOVA; 9 d later, $CD8^+$ T cell responses were analyzed (Fig. 8). Mice that were reconstituted with bone marrow cells from $CCR7^{+/+}$ mice showed an $OVA_{257–264}$-specific $CD8^+$ T cell response similar to that observed in regular $CCR7^{+/+}$ wild-type mice (as shown in Fig. 4 A). In contrast, mice that were reconstituted with $CCR7^{-/-}$ bone marrow cells demonstrated only a marginal $OVA_{257–264}$-specific $CD8^+$ T cell response. In conclusion, the experiments that are shown in Figs. 7 and 8 indicate that CCR7 expression on MHC class Ia–restricted $CD8^+$ T cells or on APCs alone is insufficient for efficient priming. Rather, CCR7 has to be expressed on T cells and APCs for effective induction of *L. monocytogenes*–specific MHC class Ia–restricted $CD8^+$ T cells.

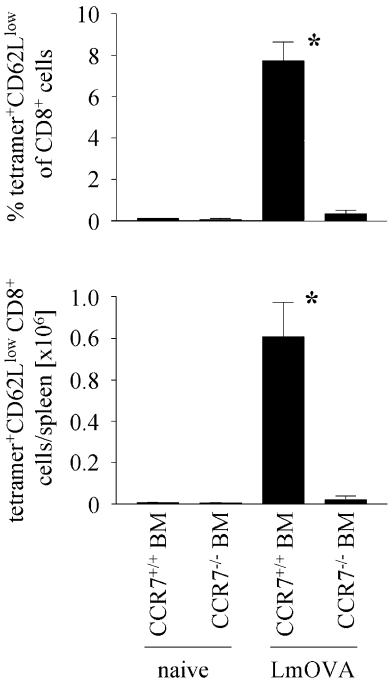

Figure 8. Expression of CCR7 on APCs is not sufficient for priming of $CD8^+$ T cells. $TCR\beta^{-/-}$ mice were irradiated and reconstituted with 10×10^6 bone marrow cells from $TCR\beta^{-/-}$ mice and 2×10^6 bone marrow cells from WT ($CCR7^{+/+}$) or KO ($CCR7^{-/-}$) mice. 8 wk after the reconstitution, mice were i.v. infected with 5×10^3 LmOVA organisms. After an additional 9 d, spleen cells were stained with FITC-conjugated anti-CD62L mAb, Cy5-conjugated anti-CD8α mAb, and PE-conjugated $OVA_{257–264}$ tetramers. Cells were analyzed by flow cytometry after addition of propidium iodide (mean ± SD of three individually analyzed mice per group). *Difference between infected mice reconstituted with $CCR7^{+/+}$ and $CCR7^{-/-}$ bone marrow was statistically significant ($P < 0.05$).

DISCUSSION

Using *L. monocytogenes* infection of $CCR7^{-/-}$ mice, we demonstrate differential requirements for the CCR7/CCR7 ligand system in the activation of different T cell subsets. Naive MHC class Ia–restricted $CD8^+$ T cells depended markedly on CCR7; MHC class Ib–restricted $CD8^+$ T cells and MHC class II–restricted $CD4^+$ T cells showed some dependency; activation of MHC class Ia–restricted $CD8^+$ memory T cells was virtually independent. The partial impairment of the T cell response also is reflected by the relative resistance of $CCR7^{-/-}$ mice during primary and secondary *L. monocytogenes* infection. Although $CCR7^{-/-}$ mice showed slightly higher *L. monocytogenes* titers at late time points of primary infection, these mice could eradicate the bacteria. Only 2 out of >100 $CCR7^{-/-}$ mice succumbed to *L. monocytogenes* during the whole series of experiments, which is similar to the normal range for wild-type mice.

The impaired $CD8^+$ T cell response was a general event that was observed for all three *L. monocytogenes*–derived MHC class Ia epitopes that were tested in our experiments ($LLO_{91–99}$, $p60_{217–225}$, and the surrogate epitope $OVA_{257–264}$). The reduction was observed in all tissues that were analyzed and at different time points following primary infection. Thus, the impaired $CD8^+$ T cell response was neither due to changes in the tissue distribution of the activated $CD8^+$ T cells, which could be anticipated from the altered distribution pattern of T cells in $CCR7^{-/-}$ mice (6), nor due to a delayed response, which had been described for $CD4^+$ T cells in *plt* mice (4). This result is in accordance with our observations in a tumor transplantation model, where $CCR7^{-/-}$ mice failed to mount a $CD8^+$ T cell response against fully allogeneic tumors (9). In contrast, Junt et al. did not detect changes of the $CD8^+$ T cell responses in *plt* mice following infection with different viruses (8). Currently, we only can speculate on the reasons for the incongruent results. Differences in the cells that are involved in $CD8^+$ T cell priming, the tissue localization of this process, and consequently, the

requirement for CCR7 between viral and bacterial infections can be anticipated. The discrepancy also could be due to the mouse strains that were used in the studies. The CCR7-deficiency results in a complete breakdown of the CCR7/CCR7 ligand system. In contrast, *plt* mice retain at least one functional copy of CCL21, the CCL21-Leu (4, 24). Despite its limited expression pattern, CCL21-Leu could be sufficient for effective priming of $CD8^+$ T cells.

In our infection model, $CCR7^{-/-}$ mice generated reduced numbers of MHC class Ia–restricted $CD8^+$ memory T cells when compared with wild-type animals. Considering the marginal primary $CD8^+$ T cell response in $CCR7^{-/-}$ mice, even this low number of $CD8^+$ memory T cells is surprising. Our results, thus, argue against a strict correlation between the strength of the primary response and the size of the memory cell population. According to current concepts, $CD8^+$ memory T cells can be divided into two major subpopulations: "effector" and "central" memory T cells (25). Effector memory T cells possess a $CCR7^-CD62L^{low}$ phenotype, are located mainly in nonlymphoid tissues, and show rapid cytokine production and cytotoxicity following activation. In contrast, central effector cells are $CCR7^+CD62L^{high}$, reside in secondary lymphoid tissues, and show delayed responses compared with effector memory T cells. Effector memory T cells most likely represent a rapidly responding cell population in the periphery, whereas central memory T cells form the basis for stable $CD8^+$ T cell memory with high proliferative capacity upon reactivation (25–28). The interrelation of both memory T cell populations is not clear, and some studies even suggest a linear differentiation pathway from $CD8^+$ effector T cells via effector memory intermediates to $CD8^+$ central memory T cells (29). In our infection model, CCR7 was dispensable for the maintenance of $CD8^+$ memory T cells and the response of these cells after challenge infection. However, this result does not challenge the current concept of central and effector memory T cells. The lack of CCR7 expression does not imply that there also is a lack of $CD8^+$ central memory T cells. It is possible that even without CCR7 expression, memory T cells can locate to niches, which allows long-term survival. Furthermore, alternative mechanisms could replace the CCR7/CCR7 ligands system. Indeed, CXCL12 can facilitate homing of memory, but not naive, T cells into secondary lymphoid tissues (30).

Despite the low number of MHC class Ia–restricted $CD8^+$ memory T cells, $CCR7^{-/-}$ mice showed virtually normal secondary $CD8^+$ T cell responses. $CD8^+$ memory T cells are responsible for rapid elimination of *L. monocytogenes* following secondary infection. A small memory T cell population controls *L. monocytogenes* less efficiently and results in a greater abundance of bacterial antigens available for T cell activation, more profound inflammation, and, consequently, a stronger secondary T cell response. Such a compensatory mechanism could explain the normal secondary $CD8^+$ T cell response that is observed in $CCR7^{-/-}$ mice. Overall, our observations allow two general conclusions: (a) the CCR7/CCR7 ligand system is not essential for generation and survival of memory T cells. Accordingly, CCR7-mediated migration of $CD8^+$ memory T cells into lymphoid tissue is not a limiting factor for persistence of memory; and (b) to a large extent, activation of $CD8^+$ memory T cells is independent of the CCR7/CCR7 ligands system. Thus, $CD8^+$ memory T cells seem to have less stringent requirements on the environment of activation.

In contrast to the $CD8^+$ T cell response to conventional MHC class Ia–restricted peptides, the response to f-met peptides presented in the context of H2-M3 was impaired only slightly by the absence of CCR7. H2-M3–restricted $CD8^+$ T cells recognize a broad range of structurally related f-met peptides, and thus, are far more promiscuous than conventional MHC class Ia–restricted $CD8^+$ T cells (31, 32). Moreover, H2-M3–restricted $CD8^+$ T cells display an activated phenotype compared with conventional $CD8^+$ T cells (33); in terms of magnitude and kinetics, H2-M3–restricted $CD8^+$ T cell responses to *L. monocytogenes* resemble secondary responses rather than primary responses (22). Therefore, H2-M3–restricted $CD8^+$ T cells could differ in their activation requirements, including a reduced dependency on mechanisms that are mediated by the CCR7/CCR7 ligand system. It also is possible that the H2-M3–restricted $CD8^+$ T cell response to *L. monocytogenes* is due, at least in part, to the activation of H2-M3–restricted $CD8^+$ memory T cells with specificities to related f-met peptides. This notion is consistent with our observations in $CCR7^{-/-}$ mice. Because $CD8^+$ memory T cell responses were largely independent of CCR7, H2-M3–restricted responses only should be impaired partially in $CCR7^{-/-}$ mice.

In comparison with the $CD8^+$ T cell response, the $CD4^+$ T cell response against *L. monocytogenes* was affected far less in $CCR7^{-/-}$ mice, and in some animals, even reached levels that were observed in control animals. Evidence for $CD4^+$ T cell responses in the absence of the CCR7/CCR7 ligands system has been described before. $CCR7^{-/-}$ and *plt* mice can generate T cell dependent antibody responses (6, 8, 9), and after immunization with ovalbumin, spleen and lymph node cells of *plt* mice proliferate and produce IL-2 in response to antigen restimulation (4). Although *plt* mice lack distinct T cell zones in spleen and lymph nodes, $CD4^+$ T cells and dendritic cells colocalize in lymphoid tissues following immunization; this allows close interactions, and, consequently, the priming of $CD4^+$ T cell responses (4). A similar scenario could be envisaged in $CCR7^{-/-}$ mice following *L. monocytogenes* infection. Naive $CD4^+$ T cells could interact with professional APCs that are loaded with *L. monocytogenes*–derived antigens outside of discrete T cell zones and result in the priming of *L. monocytogenes*–specific $CD4^+$ T cells.

Expression of CCR7 is not restricted to naive T cells. Our experiments demonstrate that neither CCR7 expression on $CD8^+$ T cells in a CCR7-negative background nor absence of CCR7 on $CD8^+$ T cells in an otherwise CCR7-

positive environment is sufficient for effective priming. Upon activation, dendritic cells express CCR7 and dendritic cell migration is impaired profoundly in CCR7$^{-/-}$ and *plt* mice. After immunization of these mice, dendritic cells fail to enter lymph nodes, and in the spleen, activated dendritic cells accumulate in the marginal zones rather than migrate into the white pulp (3, 4, 6–8). In a histologic analysis of spleens from *L. monocytogenes*–infected CCR7$^{-/-}$ mice, we detected similar alterations in dendritic cell distribution. 24 to 48 h after infection, dendritic cells entered the white pulp and accumulated in the T cell zone of wild-type mice but were trapped in the marginal zones of CCR7$^{-/-}$ mice (unpublished data). Because dendritic cells are essential for priming of CD8$^+$ T cells following *L. monocytogenes* infection (16, 17), the altered migration pattern of dendritic cells could contribute to impaired priming. We conclude that limitations in CD8$^+$ T cells and dendritic cells are responsible for the profound deficiency in the induction of MHC class Ia–restricted CD8$^+$ T cell responses in CCR7$^{-/-}$ mice.

In summary, our study demonstrates a discrete CCR7 requirement in the activation of different T cell subsets during *L. monocytogenes* infection. This result indicates that there is no general mechanism for the activation of T cells during *L. monocytogenes* infection; rather different T cell subpopulations have distinct requirements for the site and environment in which the contact between APCs and T cells takes place.

MATERIALS AND METHODS

Antibodies. Rat IgG antibodies, anti-CD16/CD32 mAb (clone: 2.4G2), anti-IFNγ mAb (R4-6A2, rat IgG1), anti-CD8α mAb (YTS169), anti-CD4 mAb (YTS191.1), anti-TCRβ mAb (H57-597), and anti-CD62L mAb (Mel-14) were purified from rat serum or hybridoma supernatants with protein G–Sepharose. Antibodies were Cy5- or FITC-conjugated according to standard protocols. Rat IgG1 isotype control mAb (clone: R3-34), anti-CD11c mAb (clone HL3, Armenian hamster), and alkaline phosphatase–conjugated rabbit anti–hamster Ig Ab were purchased from BD Biosciences.

Mice and *L. monocytogenes* infection. C57BL/6 and BALB/c and were purchased from the Bundesinstitut für Risikobewertung (BfR) in Berlin. OT1 mice (34) and TCRβ$^{-/-}$ mice (35) were bred in our facilities. CCR7$^{-/-}$ mice were crossed for six generations into the BALB/c background and for eight generations into the C57BL/6 background (6, 9). The expression of H-2K^d in CCR7$^{-/-}$ BALB/c mice was confirmed by FACS analysis. CCR7$^{-/-}$ mice were genotyped by PCR as described previously (6). All animal experiments were conducted according to the German Animal Protection Law.

Mice were infected with *L. monocytogenes* strain EGD (Lm) or with LmOVA (20). Bacteria were grown overnight in tryptic soy broth (TSB), washed twice in PBS, resuspended in PBS 10% glycerol and stored at −80°C. Aliquots were thawed and bacterial titers were determined by plating serial dilutions on TSB agar plates. For i.v. infection, *L. monocytogenes* organisms were diluted appropriately and injected in a volume of 200 μl PBS into the lateral tail veins. For i.v. infection, *L. monocytogenes* was grown overnight in TSB and washed twice in PBS. Bacterial density was determined by absorption at 600 nm and bacteria were diluted appropriately in PBS (an OD_{600} value of 1 is equivalent to 10^9 bacteria/ml). Bacteria were administered in 200 μl PBS by gastric intubation. Bacterial inocula were controlled by plating serial dilutions on TSB agar plates. For determination of bacterial burdens in organs, mice were killed, organs were homogenized in PBS, and serial dilutions of homogenates were plated on TSB agar. Colonies were counted after 24 h of incubation at 37°C.

In vitro restimulation of cells and flow cytometric determination of cytokine expression. Spleens were removed and single cell suspensions were prepared using an iron mesh sieve. Red blood cells were lysed and spleen cells were washed twice with RPMI 1640 medium supplemented with glutamine, Na-pyruvate, β-mercaptoethanol, penicillin, streptomycin, and 10% heat inactivated FCS (complete RPMI 1640 medium). Isolation of T cells from liver and tissues of the small intestine (lamina propria lymphocyte and intraepithelial lymphocytes) was performed as described previously (12). For determination of cytokine expression, 4×10^6 cells were cultured in a volume of 1 ml complete RPMI medium. Cells were stimulated for 5 h with 10^{-6} M of the peptides $LLO_{190–201}$ (NEKYAQAYPNVS), $LLO_{91–99}$ (GYKDGNEYI), $p60_{217–225}$ (KYGVSVQDI), $OVA_{257–264}$ (SIINFEKL), or a cocktail of three f-met peptides that were derived from *L. monocytogenes* proteins (fMIGWII, fMIVIL, and fMIVTLF) (10). During the final 4 h of culture, 5 μg/ml brefeldin A (Sigma-Aldrich) were added. Cultured cells were washed and incubated for 10 min with rat IgG antibodies and anti-CD16/CD32 mAb to block nonspecific antibody binding. Subsequently, cells were stained with Cy5-conjugated anti-CD4 mAb or anti-CD8α mAb, and after 30 min on ice, cells were washed with PBS and fixed for 20 min at room temperature with PBS 4% paraformaldehyde. Cells were washed with PBS 0.1% BSA, permeabilized with PBS 0.1% BSA 0.5% saponin (Sigma-Aldrich), and incubated in this buffer with rat IgG antibodies and anti-CD16/CD32 mAb. After 5 min, FITC-conjugated anti-IFNγ mAb or isotype control mAb were added. After another 20 min at room temperature, cells were washed with PBS and fixed with PBS 1% paraformaldehyde. Cells were analyzed using a FACS-Calibur and the CELLQuest software (Becton Dickinson).

Generation of MHC class I tetramers and staining of cells with tetramers. Modified forms of the full-length cDNA of H-2K^d, H-2K^b, and human β2-m were provided by D. Busch, Institute for Microbiology, Immunology, and Hygiene, Technische Universität, München, Germany. H-2K^d/LLO_{91-99} tetramers and H-2K^b/$OVA_{257–264}$ tetramers were generated as described previously (19, 36). For flow cytometry analysis, 2×10^6 cells were incubated for 15 min at 4°C with rat IgG Ab, anti-CD16/CD32 mAb, and streptavidin (Molecular Probes) in PBS 0.5% BSA 0.01% sodium azide. After incubation, cells were stained for 60 min at 4°C with Cy5-conjugated anti-CD8α mAb, FITC-conjugated anti-CD62L mAb, and PE-conjugated MHC class I-$LLO_{91–99}$ or $OVA_{257–264}$ tetramers. Subsequently, cells were washed with PBS 0.5% BSA 0.01% sodium azide and diluted in PBS. Propidium iodide was added before four-color flow cytometry analysis.

Cell transfer experiments. CD8$^+$ spleen cells from OT-1 mice were purified by magnetic cell sorting ((MACS; Miltenyi Biotec) according to the manufacturer's protocol. Subsequently, cells were washed with PBS and incubated for 4 min with 2 μM of CFSE (Molecular Probes). Cells were washed twice with complete medium, and 3–4 $\times 10^6$ cells were injected into the lateral tail vein of CCR7$^{-/-}$C57BL/6 and control C57BL/6 mice. 1 d after the adoptive transfer, mice were i.v. infected with 5×10^3 LmOVA. 3 d after infection, mice were killed, spleen cells were stained with PE-conjugated $OVA_{257–264}$ tetramers and Cy5-conjugated anti-CD8α mAb and analyzed by four-color flow cytometry after the addition of propidium iodide.

Generation of bone marrow chimeras. For the generation of mixed bone marrow chimeras, we used a protocol that was described recently by Fillatreau and Gray (23). TCRβ$^{-/-}$ mice on the C57BL/6 background were irradiated with 600 rad. Subsequently, mice were reconstituted with 10×10^6 bone marrow cells from TCRβ$^{-/-}$ mice. In addition, mice received 2×10^6 bone marrow cells from wild-type C57BL/6 mice or from CCR7$^{-/-}$ mice. Before injection, the bone marrow from wild-type and CCR7$^{-/-}$ mice was T cell depleted by MACS according to the manufacturer's protocol (CD90 depletion kit; Miltenyi Biotec). Mice were kept for

4 wk on 2 mg/ml ampicillin and 1 mg/ml neomycin sulfate in the drinking water. After 6–8 wk, reconstitution was controlled in the peripheral blood by flow cytometry. Bone marrow chimeras were infected i.v. with 5×10^3 LmOVA and analyzed 9 d later. To verify the degree of chimerism, bone marrow cells from TCR$\beta^{-/-}$ mice that were reconstituted with TCR$\beta^{-/-}$ and CCR7$^{-/-}$ bone marrow cells were isolated, and CD90$^+$ T cells were depleted by MACS. Genomic DNA from T cell–depleted bone marrow cells was prepared by phenol chloroform extraction and dissolved in water. Primers were designed to detect the intact CCR7 locus (CCR7$^+$) (forward: 5′-AGAAGAACAGCGGCGAGGA-3′, reverse: 5′-AGCATAGGCACTAGGAACCCAAA-3′) or the deficient CCR7 locus (CCR7$^-$) (forward: 5′-CAGTTTCATAGCCTGAAGAACGA-3′, reverse: 5′-GCCGATGAAGGCATACAAGAAA-3′). 10 ng of DNA from bone marrow cells of CCR7$^{-/-}$ animals were mixed with DNA from bone marrow cells of CCR7$^{+/+}$ (TCR$\beta^{-/-}$) animals at the ratios 2:1, 1:1, 1:2, 1:4, 1:8, 1:12, and 1:16. These mixtures and the DNA samples from T cell depleted bone marrow cells from the chimeras were analyzed in parallel by real-time PCR (SYBR green, ABI Prism 7000, Becton Dickinson) using the primers specific for the CCR7$^+$ and the CCR7$^-$ locus. A curve was prepared by plotting the numbers of cycle differences (ΔCT) between the two primer pairs against the mixing factor of the two DNA samples. An exponential function was fitted onto the resulting curve using Excel (Microsoft). This function (e.g., dilution $= 1.2675 \times 10^{0.8608 \times \Delta CT}$, $R^2 = 0.9995$) was used to calculate the ratio of CCR7$^+$/CCR7$^-$ DNA within T cell depleted bone marrow of reconstituted animals.

Statistical analysis. All experiments described were performed at least three times with similar results. Unless otherwise stated, experimental groups consisted of at least three mice per group, and mice were analyzed independently. For statistical analysis of frequencies and cell numbers we applied the Student's *t* test. Bacterial titers were compared using the Mann-Whitney test. Differences were considered significant with $P < 0.05$.

The authors thank Drs. D. Busch and H. Shen for providing helpful material, M. Stäber for purification of antibodies, J. Bigott and P. Mex for help with the analysis of mice, and Dr. R. Hurwitz for his support in the generation of MHC class I tetramers.

H.-W. Mittrücker, U.E. Höpken, M. Lipp, and S.H.E. Kaufmann are supported by the priority program no. SFB 633 of the German Research Foundation (DFG).

The authors have no conflicting financial interests.

Submitted: 17 June 2004
Accepted: 24 March 2005

REFERENCES

1. Müller, G., U.E. Höpken, and M. Lipp. 2003. The impact of CCR7 and CXCR5 on lymphoid organ development and systemic immunity. *Immunol. Rev.* 195:117–135.
2. Cyster, J.G. 2000. Leukocyte migration: scent of the T zone. *Curr. Biol.* 10:R30–R33.
3. Martin-Fontecha, A., S. Sebastiani, U.E. Höpken, M. Uguccioni, M. Lipp, A. Lanzavecchia, and F. Sallusto. 2003. Regulation of dendritic cell migration to the draining lymph node: impact on T lymphocyte traffic and priming. *J. Exp. Med.* 198:615–621.
4. Mori, S., H. Nakano, K. Aritomi, C.-R. Wang, M.D. Gunn, and T. Kakiuchi. 2001. Mice lacking expression of the chemokines CCL21-Ser and CCL19 (*plt* mice) demonstrate delayed but enhanced T cell immune responses. *J. Exp. Med.* 193:207–217.
5. Potsch, C., D. Vöhringer, and H. Pircher. 1999. Distinct migration patterns of naive and effector CD8 T cells in the spleen: correlation with CCR7 receptor expression and chemokine reactivity. *Eur. J. Immunol.* 29:3562–3570.
6. Förster, R., A. Schubel, D. Breitfeld, E. Kremmer, I. Renner-Müller, E. Wolf, and M. Lipp. 1999. CCR7 coordinates the primary immune response by establishing functional microenvironments in secondary lymphoid organs. *Cell.* 99:23–33.
7. Gunn, M.D., S. Kyuwa, C. Tam, T. Kakiuchi, A. Matsuzawa, L.T. Williams, and H. Nakano. 1999. Mice lacking expression of secondary lymphoid organ chemokine have defects in lymphoid homing and dendritic cell localization. *J. Exp. Med.* 189:451–460.
8. Junt, T., H. Nakano, T. Dumrese, T. Kakiuchi, B. Odermatt, R.M. Zinkernagel, H. Hengartner, and B. Ludewig. 2002. Antiviral immune responses in the absence of organized lymphoid T cell zones in plt/plt mice. *J. Immunol.* 168:6032–6040.
9. Höpken, U.E., J. Droese, J.-P. Li, J. Joergensen, D. Breitfeld, H.-G. Zerwes, and M. Lipp. 2004. The chemokine receptor CCR7 controls lymph node-dependent cytotoxic T cell priming in alloimmune responses. *Eur. J. Immunol.* 34:461–470.
10. Busch, D.H., K. Kerksiek, and E.G.P. Am. 1999. Processing of *Listeria monocytogenes* antigens and the *in vivo* T-cell response to bacterial infection. *Immunol. Rev.* 172:163–169.
11. Kaufmann, S.H.E. 2003. Immunity to intracellular bacteria. *In* Fundamental Immunology. 5th ed. W. E. Paul, editor. Lippincott-Raven, Philadelphia. 1229–1261.
12. Kursar, M., K. Bonhagen, A. Köhler, T. Kamradt, S.H.E. Kaufmann, and H.-W. Mittrücker. 2002. Organ-specific CD4$^+$ T cell response during *Listeria monocytogenes* infection. *J. Immunol.* 168:6382–6387.
13. Mittrücker, H.-W., A. Köhler, and S.H.E. Kaufmann. 2000. Substantial in vivo proliferation of CD4$^+$ and CD8$^+$ T lymphocytes during secondary *Listeria monocytogenes* infection. *Eur. J. Immunol.* 30:1053–1059.
14. Geginat, G., S. Schenk, M. Skoberne, W. Goebel, and H. Hof. 2001. A novel approach of direct *ex vivo* epitope mapping identifies dominant and subdominant CD4 and CD8 T cell epitopes from *Listeria monocytogenes*. *J. Immunol.* 166:1877–1884.
15. Lenz, L.L., E.A. Butz, and M.J. Bevan. 2000. Requirements for bone marrow-derived antigen-presenting cells in priming cytotoxic T cell responses to intracellular pathogens. *J. Exp. Med.* 192:1135–1142.
16. Jung, S., D. Unutmaz, P. Wong, G. Sano, K. De los Santos, T. Sparwasser, S. Wu, S. Vuthoori, K. Ko, F. Zavala, et al. 2002. *In vivo* depletion of CD11c$^+$ dendritic cells abrogates priming of CD8$^+$ T cells by exogenous cell-associated antigens. *Immunity.* 17:211–220.
17. Wong, P., and E.G.P. Am. 2003. Feedback regulation of pathogen-specific T cell priming. *Immunity.* 18:499–511.
18. Serbina, N.V., T.P. Salazar-Mather, C.A. Biron, W.A. Kuziel, and E.G.P. Am. 2003. TNF/iNOS-producing dendritic cells mediate innate immune defense against bacterial infection. *Immunity.* 19:59–70.
19. Busch, D.H., I.M. Pilip, S. Vijh, and E.G.P. Am. 1998. Coordinate regulation of complex T cell populations responding to bacterial infection. *Immunity.* 8:353–362.
20. Foulds, K.E., L.A. Zenewicz, D.J. Shedlock, J. Jiang, A.E. Troy, and H. Shen. 2002. Cutting edge: CD4 and CD8 T cells are intrinsically different in their proliferative responses. *J. Immunol.* 168:1528–1532.
21. Masopust, D., V. Vezys, A.L. Marzo, and L. Lefrancois. 2001. Preferential localization of effector memory cells in nonlymphoid tissue. *Science.* 291:2413–2417.
22. Kerksiek, K.M., D.H. Busch, I.M. Pilip, S.E. Allen, and E.G.P. Am. 1999. H2-M3-restricted T cells in bacterial infection: rapid primary but diminished memory responses. *J. Exp. Med.* 190:195–204.
23. Fillatreau, S., and D. Gray. 2003. D. T cell accumulation in B cell follicles is regulated by dendritic cells and is independent of B cell activation. *J. Exp. Med.* 197:195–206.
24. Nakano, H., and M.D. Gunn. 2001. Gene duplications at the chemokine locus on mouse chromosome 4: multiple strain-specific haplotypes and the deletion of secondary lymphoid-organ chemokine and EBI-1 ligand chemokine genes in the *plt* mutation. *J. Immunol.* 166:361–369.
25. Sallusto, F., J. Geginat, and A. Lanzavecchia. 2004. Central and effector memory T cell subsets: function, generation, and maintenance. *Annu. Rev. Immunol.* 22:745–763.
26. Northrop, J.K., and H. Shen. 2004. CD8$^+$ T-cell memory: only the good ones last. *Curr. Opin. Immunol.* 16:451–455.
27. Masopust, D., and L. Lefrancois. 2003. CD8 T-cell memory: the other half of the story. *Microbes Infect.* 5:221–226.
28. Masopust, D., S. Kaech, J.E. Wherry, and R. Ahmed. 2004. The role of programming in memory T-cell development. *Curr. Opin. Immunol.* 16:217–225.

29. Wherry, J.E., V. Teichgräber, T.C. Becker, D. Masopust, S.M. Kaech, R. Antia, U. von Andrian, and R. Ahmed. 2003. Lineage relationship and protective immunity of memory CD8 T cell subsets. *Nat. Immunol.* 4:225–234.
30. Scimone, M.L., T.W. Felbinger, I.B. Mazo, J.V. Stein, U.H. von Andrian, and W. Weninger. 2004. CXCL12 mediates CCR7-independent homing of central memory cells, but not naive T cells, in peripheral lymph nodes. *J. Exp. Med.* 199:1113–1120.
31. Rolph, M.S., and S.H.E. Kaufmann. 2000. Partially TAP-independent protection against *Listeria monocytogenes* by H2-M3-restricted $CD8^+$ T cells. *J. Immunol.* 165:4575–4580.
32. Ploss, A., G. Lauvau, B. Contos, K.M. Kerksiek, P.D. Guirnalda, I. Leiner, M.J. Bevan, and E.G.P. Am. 2003. Promiscuity of MHC class Ib-restricted T cell responses. *J. Immunol.* 171:5948–5955.
33. Urdahl, K.B., J.C. Sun, and M.J. Bevan. 2002. Positive selection of MHC class Ib-restricted cells on hematopoietic cells. *Nat. Immunol.* 3:772–779.
34. Hogquist, K.A., S.C. Jameson, W.R. Heath, J.L. Howard, M.J. Bevan, and F.R. Carbone. 1994. T cell receptor antagonist peptides induce positive selection. *Cell.* 14:17–27.
35. Mombaerts, P., A.R. Clarke, M.A. Rudnicki, J. Iacomini, S. Itohara, J.J. Lafaille, L. Wang, Y. Ichikawa, R. Jaenisch, M.L. Hooper, and S. Tonegawa. 1992. Mutation in T-cell antigen receptor genes α and β block thymocyte development at different stages. *Nature.* 360:225–231.
36. Mittrücker, H.-W., M. Kursar, A. Köhler, R. Hurwitz, and S.H.E. Kaufmann. 2001. Role of CD28 for the generation and expansion of antigen-specific $CD8^+$ T lymphocytes during infection with *Listeria monocytogenes*. *J. Immunol.* 167:5620–5627.